# Camouflage thermotics: A cavity without disturbing heat signatures outside

Liujun Xu, Ruizhe Wang, and Jiping Huang

Citation: Journal of Applied Physics **123**, 245111 (2018); doi: 10.1063/1.5034183
View online: https://doi.org/10.1063/1.5034183
View Table of Contents: http://aip.scitation.org/toc/jap/123/24
Published by the American Institute of Physics

# Camouflage thermotics: A cavity without disturbing heat signatures outside

Liujun Xu, Ruizhe Wang, and Jiping Huang[a)]
*Department of Physics, State Key Laboratory of Surface Physics, and Key Laboratory of Micro and Nano Photonic Structures (MOE), Fudan University, Shanghai 200433, China and Collaborative Innovation Center of Advanced Microstructures, Nanjing 210093, China*

(Received 10 April 2018; accepted 7 June 2018; published online 26 June 2018)

Cloaks can protect objects without disturbing heat signatures outside cloaks, and hence, objects are invisible to outside detection. However, cloaks themselves are visible to inside detection because they possess different heat signatures from the outside. This fact limits applications. Here, we solve this problem in thermotics by developing a different theory and then propose the scheme of thermal supercavity, a cavity without disturbing heat signatures outside. We investigate different supercavities with various shapes in two or three dimensions and validate the desired effects by simulations and experiments. We further design the scheme of super-invisibility which makes the cavity itself also invisible to inside detection. Moreover, our scheme simplifies the complicated parameters of non-circle shaped cloaks, which requires only two natural materials with a simple layer structure. Our work is useful for achieving new kinds of thermal devices, including thermal camouflage and designing similar supercavities in magnetostatics, electrostatics, particle diffusion, etc. *Published by AIP Publishing.* https://doi.org/10.1063/1.5034183

## I. INTRODUCTION

Invisibility is a long-standing dream of human beings. Since the theory of transformation optics was put forward,[1,2] electromagnetic invisibility has attracted much attention (e.g., see Refs. 3–5). In the duration, the physical fields have also been extended from those described by wave equations (say, in electromagnetics/optics[1–5] and acoustics[6,7]) to those determined by diffusion equations (e.g., in thermotics[8–10]). Furthermore, the theories have been developed from the original transformation optics to others (e.g., directly solving the Laplace equation[11–20]), in order to design practical structures.

However, the existing thermal cloaks[12–14,21,22] are faced with a common problem: cloaks themselves are visible to inside detection. Let us take a thermal cloak (designed by transformation thermotics) as an example; see Fig. 1(a). The thermal cloak (a shell surrounding the cavity) can guide heat to flow around the cavity (in which arbitrary objects can be placed) without disturbing heat signatures outside the cloak (or in the background). Thus, objects located in the cavity are "invisible" to outside detection [Fig. 1(a)]. However, thermal cloaks themselves are "visible" to inside detection [Fig. 1(a)] since they have different heat signatures from the outside as determined by the associated theories (say, the theory of transformation thermotics).[21,22] This fact limits applications, e.g., in the cases of misleading infrared detection.

To solve this problem, here we establish a different theory, which allows us to propose the scheme of the supercavity as schematically shown in Figs. 1(b) and 1(c). Clearly, the cavity does not disturb external heat signatures including those in the region of the shell.

We further design the super-invisibility which makes both the shell and cavity invisible to inside detections. Therefore, as pioneered by the work in Ref. 16, the whole system is invisible to whatever detections, which will contribute to thermal camouflage or illusion.[15,16,23–25]

The aforementioned behaviors will be confirmed by simulations and experiments in this work. To proceed, let us first present the theory.

## II. THEORY

We start by presenting the Fourier law that governs the process of heat conduction

$$\boldsymbol{J} = -\kappa \nabla T, \tag{1}$$

where $\boldsymbol{J}$, $\kappa$, and $T$ are heat flux, thermal conductivity, and temperature, respectively.

As shown in Figs. 1(b)–1(d), our system contains three parts: shell (constructed by anisotropic materials in this work), cavity (in which arbitrary objects can be placed), and background. Comparing with traditional cloaks where temperature fields are distorted in the shell [Fig. 1(a)], we expect to keep the temperature fields of both the shell and background the same [Figs. 1(b) and 1(c)], no matter what kinds of objects are placed in the cavity. In fact, if we can artificially match the boundary conditions (temperature $T$ and normal heat flux $\boldsymbol{J}$) between the shell and background, our expectation could be achieved indeed. In what follows, we give a proof to verify our idea.

Let us consider the background with two solutions of temperatures ($T'$ and $T''$) and heat fluxes ($\boldsymbol{J}'$ and $\boldsymbol{J}''$) and introduce an auxiliary function $\boldsymbol{Z}(\boldsymbol{r}) = (T' - T'')(\boldsymbol{J}' - \boldsymbol{J}'')$. Supposing that we have artificially matched the boundary conditions between the background and the shell

$$\begin{aligned} T'_{\Sigma} &= T''_{\Sigma} \\ (\boldsymbol{J}' \cdot \boldsymbol{e}_n)_{\Sigma} &= (\boldsymbol{J}'' \cdot \boldsymbol{e}_n)_{\Sigma}, \end{aligned} \tag{2}$$

[a)]Electronic mail: jphuang@fudan.edu.cn

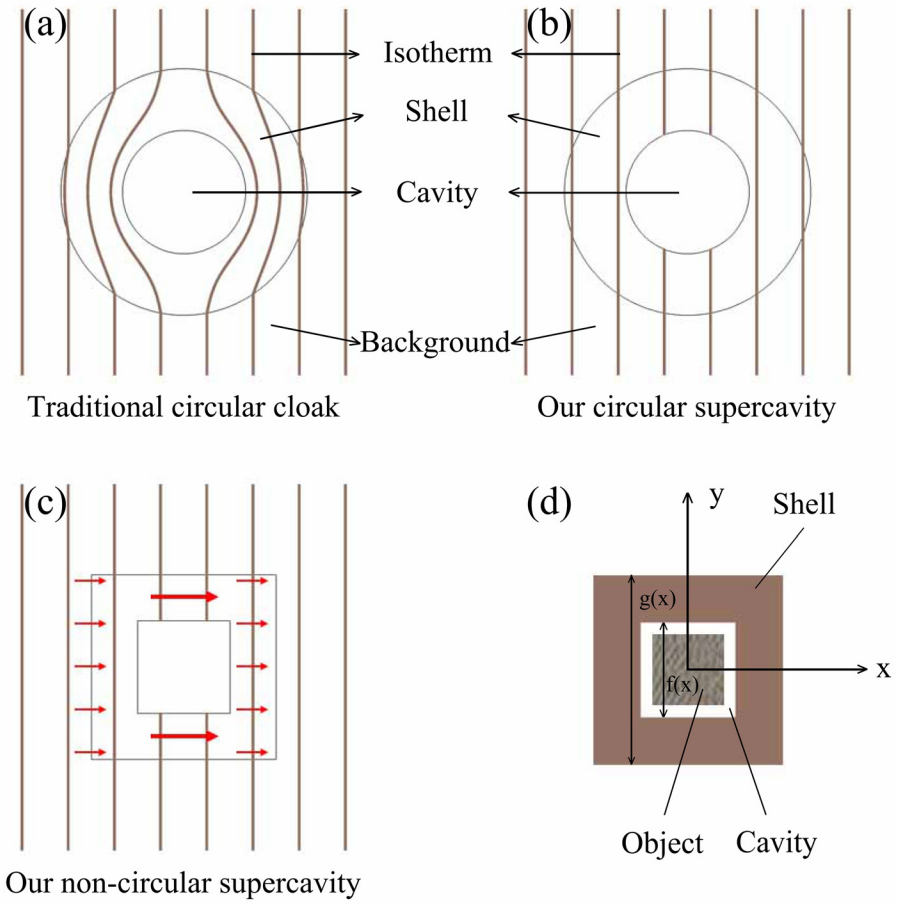


FIG. 1. Schematic diagram showing our concept: (a) the traditional circular cloak contains a distorted temperature field in the shell, thus causing the shell to be "visible" to inside thermal detection; (b) our circular supercavity proposed in this work has an undistorted temperature field in the shell, thus yielding the shell to be "invisible". Besides the circular case depicted in (b), our supercavity can be non-circular as well: (c) shows an example of square supercavity, whose details are indicated in (d). Brown lines and red arrows represent isotherms and heat flux, respectively.

where $\Sigma$ represents the boundary and $\boldsymbol{e}_n$ is the unit normal vector of the boundary. So the integral value of $\boldsymbol{Z}(\boldsymbol{r})$ on the boundary $\Sigma$ must be zero

$$\int_{\Sigma} \boldsymbol{Z}(\boldsymbol{r}) \cdot \mathrm{d}\boldsymbol{s} = \int_{V} \nabla \cdot \boldsymbol{Z}(\boldsymbol{r}) \mathrm{d}\tau = 0. \tag{3}$$

We then calculate the divergence of $\boldsymbol{Z}(\boldsymbol{r})$

$$\begin{aligned} \nabla \cdot \boldsymbol{Z}(\boldsymbol{r}) = (\nabla T' - \nabla T'') \cdot (\boldsymbol{J}' - \boldsymbol{J}'') + (T' - T'') \\ \cdot (\nabla \cdot \boldsymbol{J}' - \nabla \cdot \boldsymbol{J}''). \end{aligned} \tag{4}$$

For the same background, we obtain

$$\nabla \cdot \boldsymbol{J}' = \nabla \cdot \boldsymbol{J}'' = q, \tag{5}$$

where $q$ is the energy generated per unit volume and per unit time. Then, Eq. (4) becomes

$$\nabla \cdot \boldsymbol{Z}(\boldsymbol{r}) = (\nabla T' - \nabla T'') \cdot (\boldsymbol{J}' - \boldsymbol{J}''). \tag{6}$$

Equation (3) reads

$$\int_{V} (\nabla T' - \nabla T'') \cdot (\boldsymbol{J}' - \boldsymbol{J}'') \mathrm{d}\tau = 0. \tag{7}$$

We further reduce Eq. (7) according to Eq. (1)

$$-\int_{V} \kappa (\nabla T' - \nabla T'')^2 \mathrm{d}\tau = 0. \tag{8}$$

Since $\kappa$ is always positive, we achieve

$$\nabla T' = \nabla T''. \tag{9}$$

Then, we can conclude that if one can match the boundary conditions between the background and shell, the temperature profile of the background can remain unchanged. To match the boundary conditions between the background and shell, we can design the temperature distribution as follows:

$$\begin{aligned} (\text{Gradient}\, T)_x &= \nabla T_0, \\ (\text{Gradient}\, T)_y &= 0, \end{aligned} \tag{10}$$

where $(\text{Gradient}\, T)_x$ (or $(\text{Gradient}\, T)_y$) is the horizontal (or vertical) thermal gradient in the shell and $\nabla T_0$ is the thermal gradient in the background. We do not consider the boundary conditions of heat flux because the normal heat flux is zero; see red arrows in Fig. 1(c).

Now, we need to design the parameters of the shell to satisfy the required temperature distribution [Eq. (10)]. According to the conservation of heat flux in the shell; see red arrows in Fig. 1(c), we obtain

$$\begin{aligned} -\kappa_{xx}[g(x) - f(x)]|(\text{Gradient}\, T)_x| &= -\kappa_b g(x)|\nabla T_0|, \\ -\kappa_{yy}|(\text{Gradient}\, T)_y| &= \delta, \end{aligned} \tag{11}$$

where $\delta$ should be a non-zero (finite) variable, and $\kappa_{xx}$ (or $\kappa_{yy}$) is the horizontal (or vertical) thermal conductivity of the shell (or anisotropic material), and $\kappa_b$ is the thermal conductivity of

background. $f(x)$ and $g(x)$ describe the length of the cavity and shell at the position $x$, respectively, which have been depicted in Fig. 1(d). Then, we derive the thermal conductivity $\kappa_{ani1}$ of the shell (anisotropic material) as

$$\kappa_{ani1} = \begin{pmatrix} \dfrac{g(x)\kappa_b}{g(x)-f(x)} & 0 \\ 0 & \kappa_{yy} \end{pmatrix}, \tag{12}$$

where $\kappa_{yy}$ should be $\infty$ to ensure a non-zero $\delta$. Equation (12) just helps to design our desired shell which itself is also invisible; see Figs. 2–4.

Moreover, our theory can even make the cavity invisible (say, super-invisibility) with some sacrifice; see Fig. 5. The cloak designed according to Eq. (12) works regardless of the change of objects in the cavity. However, if we expect to make the cavity also invisible, the shell should be designed according to the cavity (object). We can design as follows.

Similar to the scheme of the supercavity (the conservation of heat flux), we obtain

$$\begin{aligned} \{-\kappa_{xx}[n(x)-m(x)]-\kappa_c m(x)\}|(\text{Gradient } T)_x| &= -\kappa_b n(x)|\nabla T_0|, \\ -\kappa_{yy}|(\text{Gradient } T)_y| &= \delta, \end{aligned} \tag{13}$$

where $m(x)$ and $n(x)$ are the length of the cavity and shell, which have been depicted in Fig. 5(a). Then, we derive the thermal conductivity $\kappa_{ani2}$ of the shell (or anisotropic material)

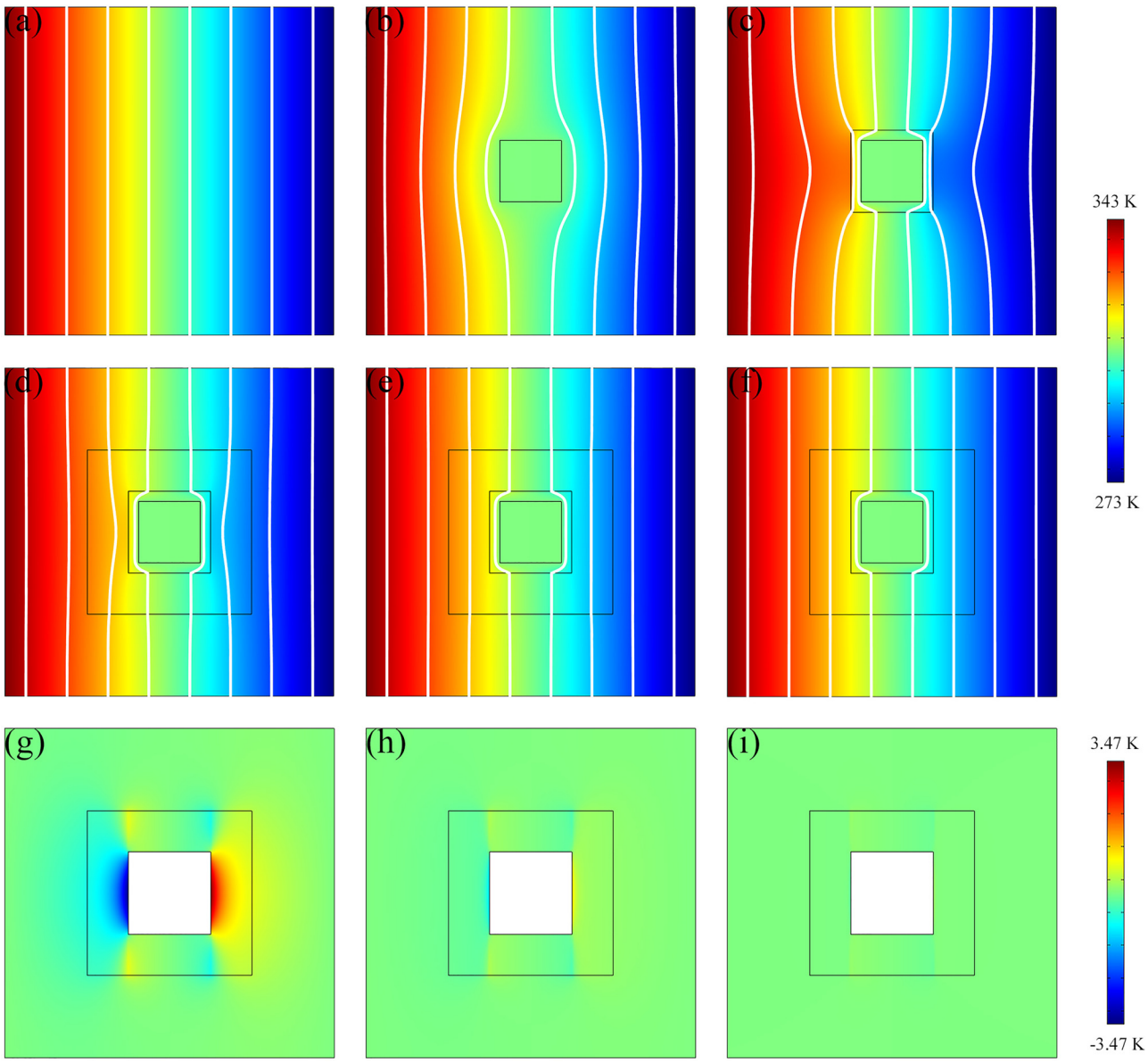


FIG. 2. Simulations of the square shaped cavity: the color surface displays the distribution of temperature (a)–(f) or temperature difference (g)–(i), and the white lines in (a)–(f) represent the isotherms. (a) background material (silica gel) with thermal conductivity 3.6 W/(m · K) and size 8 × 8 cm; (b) the same background material whose central square area is occupied by an object (red copper) with 397 W/(m · K) and 1.5 × 1.5 cm; (c) same as (b), but the object is wrapped in air with 0.026 W/(m · K) and 2 × 2 cm. (d)–(f) are same as (c), but the air is further wrapped in a square shell (that is constructed by an anisotropic material) with 4 × 4 cm. For the square shell (or the anisotropic material), the thermal conductivity is determined according to Eq. (12): $\kappa_{yy} = 20$ (d), 200 (e), and 2000 (f) W/(m · K). The temperature difference between (d)–(f) and (a) is shown in (g)–(i), respectively. In (g)–(i), the central white square with 2 × 2 cm denotes the area involving both the object and air in (d)–(f); this area just corresponds to the cavity as indicated in Fig. 1.

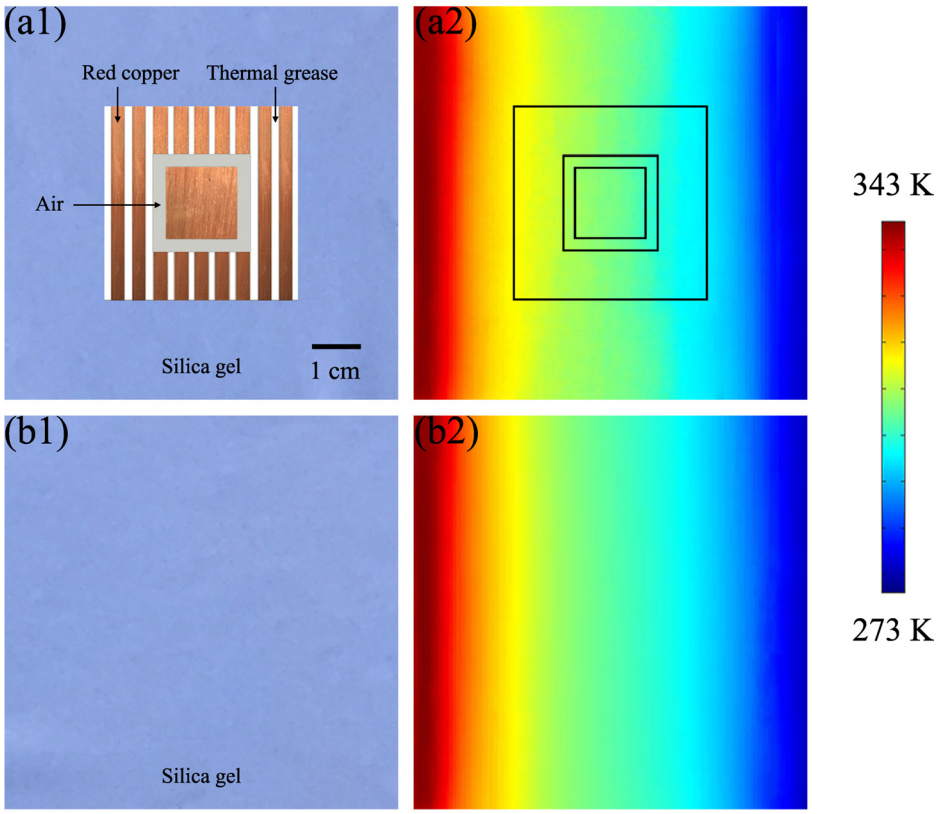


FIG. 3. Experiments of square shaped cavity: thermal images of experimental samples (a1) and (b1) are displayed in (a2) and (b2), respectively. (a1) is the fabricated sample which is composed of a middle square (red copper) with size $1.5 \times 1.5$ cm; out of the middle square is air with $2 \times 2$ cm; out of the air is the shell composed of the anisotropic material with $4 \times 4$ cm, which is made up of red copper and thermal grease; outermost is the background (silica gel) with $8 \times 8$ cm. (b1) shows the sample of uniform background, namely, silica gel. Thermal conductivities of red copper, thermal grease, air, and silica gel are 397, 1.6, 0.026, and 3.6 W/(m · K), respectively; the thickness of the two samples is about 0.3 mm.

$$\kappa_{ani2} = \begin{pmatrix} \dfrac{n(x)\kappa_b - m(x)\kappa_c}{n(x) - m(x)} & 0 \\ 0 & \kappa_{yy} \end{pmatrix}, \tag{14}$$

where $\kappa_{yy}$ should also be $\infty$ and $\kappa_c$ is the thermal conductivity of cavity (object).

## III. SIMULATIONS AND EXPERIMENTS OF THE SQUARE SHAPED CAVITY

We perform finite-element simulations based on the commercial software COMSOL Multiphysics (http://www.comsol.com/) to show the validation of the aforementioned theory. Without loss of generality, we take the square shape as an example and display the simulations in Figs. 2(a)–2(f). Figure 2(a) shows the homogeneous background with uniform thermal field. Then, we put an object (whose thermal conductivity is different from the background) into the background, and the temperature profile is distorted; see Fig. 2(b). To remove the distortion, we add air outside the object to construct an insulation cavity [Fig. 2(c)]. However, the thermal profile is still not recovered; see Fig. 2(c). In Figs. 2(d)–2(f), three shells (anisotropic materials) with $\kappa_{yy} = 20,200$ and 2000 W/(m · K) according to Eq. (12) are applied to remove the temperature distortion. Figures 2(d)–2(f) exhibit almost the same temperature profile as that in Fig. 2(a); certainly larger $\kappa_{yy}$ yields better comparison, which echoes with the prediction of Eq. (12). So the object is well hidden and the shell itself is also invisible. We further calculate the difference between Figs. 2(a) and 2(d)–2(f); see Figs. 2(g)–2(i). Clearly, the temperature distortion in the shell is well removed, especially for the case of larger $\kappa_{yy}$.

On the other hand, we also fabricated two samples [Figs. 3(a1) and 3(b1)] to verify the simulation results in Fig. 2. The anisotropic thermal conductivity of the shell, which is determined by Eq. (12), is designed with layer structures

$$\kappa = \begin{pmatrix} \dfrac{(a/b+1)\kappa_a\kappa_b}{(a/b)\kappa_b + \kappa_a} & 0 \\ 0 & \dfrac{(a/b)\kappa_a + \kappa_b}{a/b+1} \end{pmatrix}, \tag{15}$$

where $a$ (or $b$) is the length of the uniform material with thermal conductivity $\kappa_a$ (or $\kappa_b$).

Then, we choose red copper and thermal grease with an appropriate ratio according to Eq. (15) to fabricate the shell and we utilize silica gel as the background material [Fig. 3(a1)]. Figure 3(a2) is the measured result of the sample shown in Fig. 3(a1). Figures 3(b1) and 3(b2) show a reference group. Figure 3(b2) is the experimental result of the homogeneous background shown in Fig. 3(b1). Clearly, the comparison between Figs. 3(a2) and 3(b2) is satisfactory. A small difference between experiments and simulations is caused by the thermal convection, and the experiments show the qualitative results.

## IV. SIMULATIONS OF VARIOUS SHAPED CAVITIES IN TWO OR THREE DIMENSIONS

To show the robustness and generality of our theory, we further perform simulations for other shapes like rectangle, circle, ellipse, and irregular shape in two dimensions; we

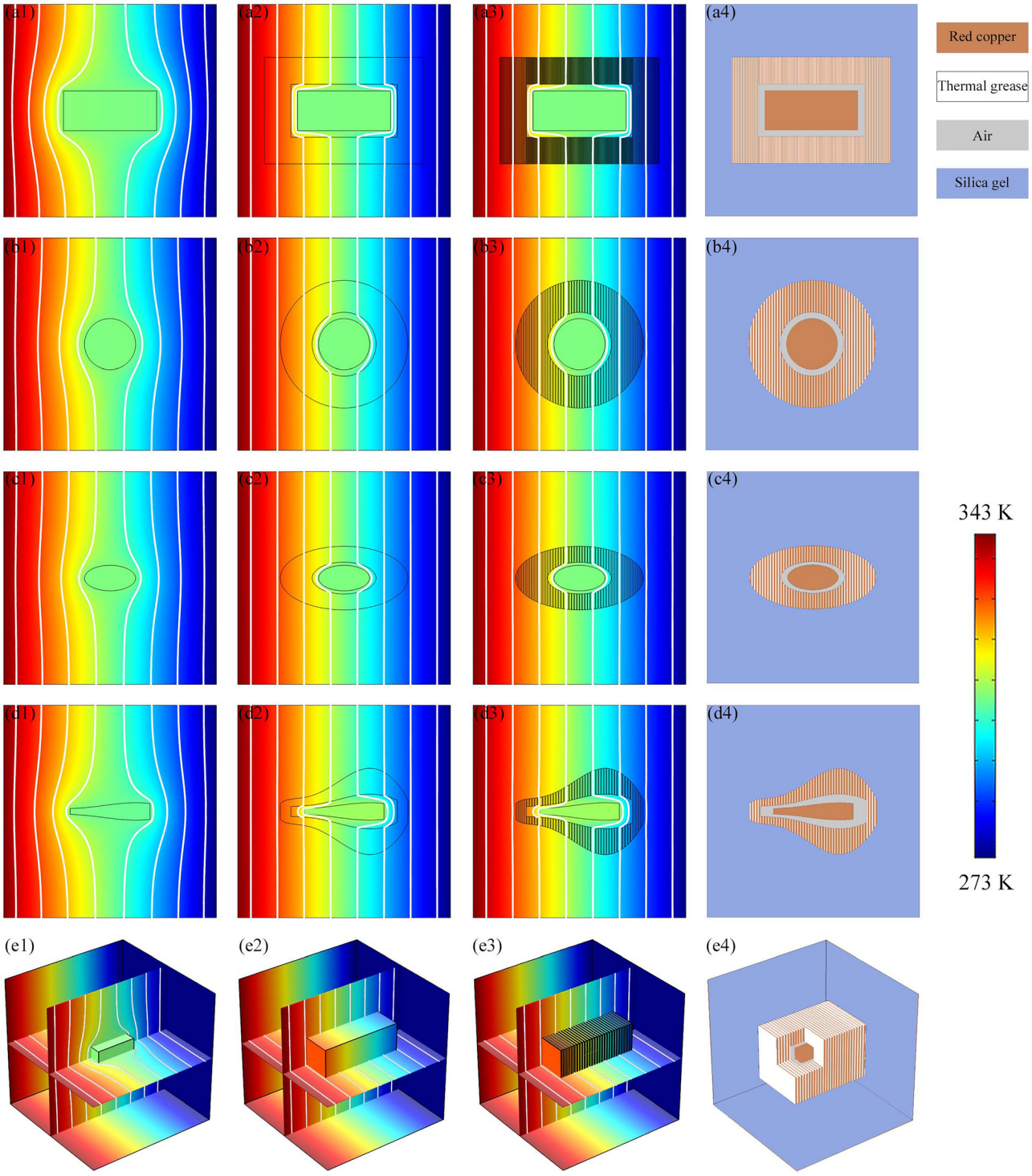


FIG. 4. Simulations of various shaped cavities. (a1)–(a4) show a rectangular case: (a1) and (a2) are, respectively, the same as Figs. 2(b) and 2(f), but for the rectangular shape; for experimentally demonstrating (a2), (a3) shows simulation results of the structure designed in (a4) according to Fig. 3 and Eq. (15). Similar to (a1)–(a4), (b1)–(b4) show the circular shape, (c1)–(c4) the elliptic shape, (d1)–(d4) the irregular shape, and (e1)–(e4) the cuboid shape. For clarity, a small cuboid in the middle of (e4) is removed to display the inner structure. The results (namely, the uniform thermal gradients in shells) obtained from this figure are independent of sizes of the shells due to the generality of Eqs. (12) and (15). Thus here we omit such specific values of sizes adopted for simulation.

also investigate the shape of a three-dimensional cuboid. See Fig. 4. In Figs. 4(a1)–4(e1), we place the objects with the shapes of rectangle, circle, ellipse, irregular shape, and cuboid into the thermal field, respectively. As a result, the temperature profile is undoubtedly distorted. Then, we put these objects into the cavity associated with the shells [designed according to Eq. (12) where $\kappa_{yy} = 2000$ W/(m · K)]; see Figs. 4(a2)–4(e2) that show the desired effects (namely, the temperature gradient in the shell is the same as that in the background). Figures 4(a3)–4(e3) show the simulation results of the practical structures displayed in Figs. 4(a4)–4(e4), respectively. The parameters of these structures are determined according to Eq. (15). The simulation

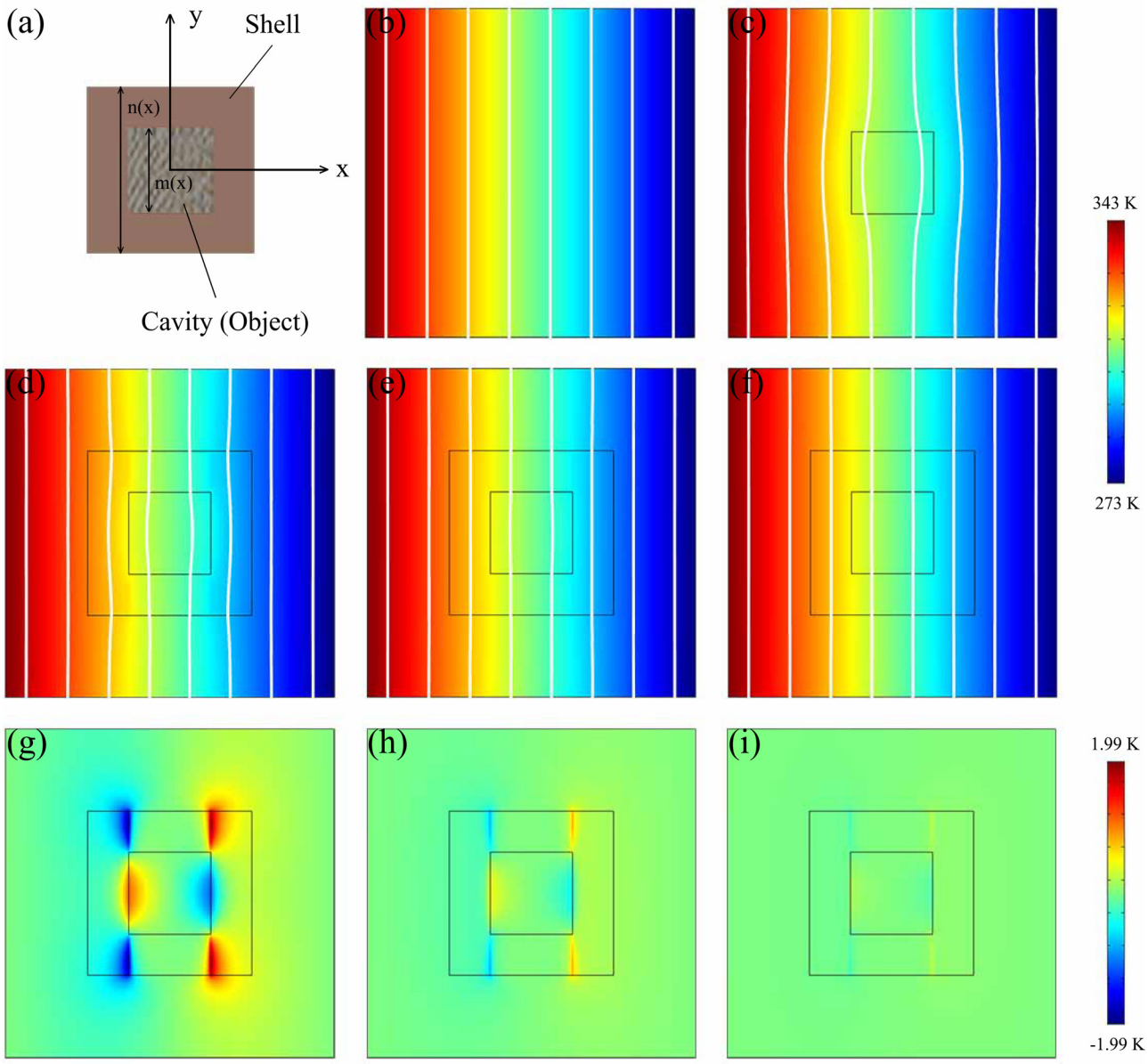


FIG. 5. Simulations of super-invisibility. (a) schematic diagram of the design; (b) background material (silica gel) with thermal conductivity 3.6 W/(m · K) and size $8 \times 8$ cm; (c) the same background material whose central square area is occupied by an object with 7 W/(m · K) and $2 \times 2$ cm; (d)–(f) the same as (b), but the object is wrapped in a square shell (that is constructed by an anisotropic material) with $4 \times 4$ cm. For the square shell, the thermal conductivity is determined according to Eq. (14): $\kappa_{yy} = 20$ (d), 200 (e), and 2000 W/(m · K) (f). The temperature difference between (d)–(f) and (b) is shown in (g)–(i), respectively.

results show that the shells themselves are invisible indeed, while the objects are hidden in the central regions.

## V. SIMULATIONS OF SUPER-INVISIBILITY

Similar simulations with Fig. 2 are also conducted to validate the super-invisibility; see Fig. 5. The cavity is fully filled with objects, and there is no longer insulation material (air) between the object and shell. Therefore, the shell is specific, which only works for a certain object. Figure 5(b) shows a uniform thermal field in the homogeneous background. Then, we put an object into the background; see Fig. 5(c). In Figs. 5(d)–5(f), three shells with $\kappa_{yy} = 20, 200$ and 2000 W/(m · K) according to Eq. (14) are applied to cancel out the temperature distortion. We also calculate the difference between Figs. 5(b) and 5(d)–5(f); see Figs. 5(g)–5(i). Clearly, the temperature distortion in the shell and cavity is both removed indeed, and hence, super-invisibility is realized.

## VI. DISCUSSION AND CONCLUSION

Our supercavity is essentially a unidirectional passive cloak, for the boundary conditions are artificially matched. If the cavity is rotated or uniform external field is changed, our scheme does not work again. Compared with the existing unidirectional active cloak,[26–28] our scheme does not require extra sources, which is no doubt more applicable.

Our scheme also simplifies the extremely complicated parameters of non-circle shaped cloaks. As designed by transformation thermotics,[10] non-circle shaped cloaks require extreme materials including inhomogeneity, anisotropy, and

singularity, which are almost impossible to experimentally realize regardless of the development of thermal metamaterials. In contrast, our design requires only two natural materials with a simple layer structure, which will bring great convenience and potential applications.

We have investigated the case of steady states only. Certainly, the unsteady state is subjected to further research because of the specific role of heat capacity.[10,29]

So far, we have established a theory and then proposed the scheme of the thermal supercavity which makes the shell itself also invisible to inside detection. The effect has been confirmed in simulations and experiments. Only two natural materials (red copper and thermal grease, which are commercially available) were used to fabricate the shell in our experiment, which overcomes parameter complexity. Our theory is general for designing different shaped shells in both two and three dimensions. We also design the super-invisibility which makes the whole system invisible to whatever detections.

Our scheme enriches the research scale of thermal devices including thermal camouflage. It is useful for directly designing similar supercavities and super-invisibility in disciplines like magnetostatics,[11] electrostatics,[30] and particle diffusion,[31] where electric conductivities, magnetic permeabilities, and diffusion coefficients, respectively, play the same role as thermal conductivities in thermotics.

## ACKNOWLEDGMENTS

We acknowledge the financial support from the National Natural Science Foundation of China under Grant No. 11725521 and from the Science and Technology Commission of Shanghai Municipality under Grant No. 16ZR1445100.

[1]J. B. Pendry, D. Schurig, and D. R. Smith, "Controlling electromagnetic fields," Science **312**, 1780 (2006).
[2]U. Leonhardt, "Optical conformal mapping," Science **312**, 1777 (2006).
[3]D. Schurig, J. J. Mock, B. J. Justice, S. A. Cummer, J. B. Pendry, A. F. Starr, and D. R. Smith, "Metamaterial electromagnetic cloak at microwave frequencies," Science **314**, 977 (2006).
[4]R. Liu, C. Ji, J. J. Mock, J. Y. Chin, T. J. Cui, and D. R. Smith, "Broadband ground-plane cloak," Science **323**, 366 (2009).
[5]T. Ergin, N. Stenger, P. Brenner, J. B. Pendry, and M. Wegener, "Three-dimensional invisibility cloak at optical wavelengths," Science **328**, 337 (2010).
[6]H. Y. Chen and C. T. Chan, "Acoustic cloaking in three dimensions using acoustic metamaterials," Appl. Phys. Lett. **91**, 183518 (2007).
[7]S. Zhang, C. Xia, and N. Fang, "Broadband acoustic cloak for ultrasound waves," Phys. Rev. Lett. **106**, 024301 (2011).
[8]C. Z. Fan, Y. Gao, and J. P. Huang, "Shaped graded materials with an apparent negative thermal conductivity," Appl. Phys. Lett. **92**, 251907 (2008).
[9]T. Y. Chen, C.-N. Weng, and J.-S. Chen, "Cloak for curvilinearly anisotropic media in conduction," Appl. Phys. Lett. **93**, 114103 (2008).
[10]S. Guenneau, C. Amra, and D. Veynante, "Transformation thermodynamics: Cloaking and concentrating heat flux," Opt. Express **20**, 8207 (2012).
[11]F. Gömöry and A. Sanchez, "Experimental realization of a magnetic cloak," Science **335**, 1466 (2012).
[12]H. Y. Xu, X. H. Shi, F. Gao, H. D. Sun, and B. L. Zhang, "Ultrathin three-dimensional thermal cloak," Phys. Rev. Lett. **112**, 054301 (2014).
[13]T. C. Han, X. Bai, D. L. Gao, J. T. L. Thong, B. W. Li, and C.-W. Qiu, "Experimental demonstration of a bilayer thermal cloak," Phys. Rev. Lett. **112**, 054302 (2014).
[14]Y. G. Ma, Y. C. Liu, M. Raza, Y. D. Wang, and S. L. He, "Experimental demonstration of a multiphysics cloak: Manipulating heat flux and electric current simultaneously," Phys. Rev. Lett. **113**, 205501 (2014).
[15]T. C. Han, X. Bai, J. T. L. Thong, B. W. Li, and C.-W. Qiu, "Full control and manipulation of heat signatures: Cloaking, camouflage and thermal metamaterials," Adv. Mater. **26**, 1731 (2014).
[16]T. Z. Yang, X. Bai, D. L. Gao, L. Z. Wu, B. W. Li, J. T. L. Thong, and C.-W. Qiu, "Invisible sensors: Simultaneous sensing and camouflaging in multiphysical fields," Adv. Mater. **27**, 7752 (2015).
[17]S. Yang, L. J. Xu, R. Z. Wang, and J. P. Huang, "Full control of heat transfer in single-particle structural materials," Appl. Phys. Lett. **111**, 121908 (2017).
[18]R. Z. Wang, L. J. Xu, and J. P. Huang, "Thermal imitators with single directional invisibility," J. Appl. Phys. **122**, 215107 (2017).
[19]L. J. Xu, C. R. Jiang, J. Shang, R. Z. Wang, and J. P. Huang, "Periodic composites: Quasi-uniform heat conduction, Janus thermal illusion, and illusion thermal diodes," Euro. Phys. J. B **90**, 221 (2017).
[20]R. Z. Wang, L. J. Xu, Q. Ji, and J. P. Huang, "A thermal theory for unifying and designing transparency, concentrating and cloaking," J. Appl. Phys. **123**, 115117 (2018).
[21]S. Narayana and Y. Sato, "Heat flux manipulation with engineered thermal materials," Phys. Rev. Lett. **108**, 214303 (2012).
[22]R. Schittny, M. Kadic, S. Guenneau, and M. Wegener, "Experiments on transformation thermodynamics: Molding the flow of heat," Phys. Rev. Lett. **110**, 195901 (2013).
[23]R. Hu, X. L. Wei, J. Y. Hu, and X. B. Luo, "Local heating realization by reverse thermal cloak," Sci. Rep. **4**, 3600 (2014).
[24]R. Hu, S. Zhou, Y. Li, D. Y. Lei, X. B. Luo, and C.-W. Qiu, "Illusion thermotics," Adv. Mater. **30**, 1707237 (2018).
[25]Y. Li, X. Bai, T. Z. Yang, H. Luo, and C.-W. Qiu, "Structured thermal surface for radiative camouflage," Nat. Commun. **9**, 273 (2018).
[26]Q. Ma, Z. L. Mei, S. K. Zhu, T. Y. Jin, and T. J. Cui, "Experiments on active cloaking and illusion for Laplace equation," Phys. Rev. Lett. **111**, 173901 (2013).
[27]D. M. Nguyen, H. Y. Xu, Y. M. Zhang, and B. L. Zhang, "Active thermal cloak," Appl. Phys. Lett. **107**, 121901 (2015).
[28]C. W. Lan, K. Bi, Z. H. Gao, B. Li, and J. Zhou, "Achieving bifunctional cloak via combination of passive and active schemes," Appl. Phys. Lett. **109**, 201903 (2016).
[29]T. Z. Yang, Y. Su, W. Xu, and X. D. Yang, "Transient thermal camouflage and heat signature control," Appl. Phys. Lett. **109**, 121905 (2016).
[30]F. Yang, Z. L. Mei, T. Y. Jin, and T. J. Cui, "DC electric invisibility cloak," Phys. Rev. Lett. **109**, 053902 (2012).
[31]S. Guenneau and T. M. Puvirajesinghe, "Fick's second law transformed: One path to cloaking in mass diffusion," J. R. Soc. Interface **10**, 20130106 (2013).